arXiv:cond-mat/0410093v3 [cond-mat.supr-con] 29 Dec 2004

Self-field effects upon the critical current density of flat superconducting strips

Ali A. Babaei Brojeny
Department of Physics, Isfahan University of Technology,
Isfahan 84154, Iran, and Department of Physics and Astronomy,
Iowa State University, Ames, Iowa, 50011–3160

John R. Clem
Ames Laboratory and Department of Physics and Astronomy,
Iowa State University, Ames, Iowa, 50011–3160

(Dated: February 2, 2008)

We develop a general theory to account self-consistently for self-field effects upon the average transport critical current density J_c of a flat type-II superconducting strip in the mixed state when the bulk pinning is characterized by a field-dependent depinning critical current density $J_p(\boldsymbol{B})$, where $\boldsymbol{B}$ is the local magnetic flux density. We first consider the possibility of both bulk and edge-pinning contributions but conclude that bulk pinning dominates over geometrical edge-barrier effects in state-of-the-art YBCO films and prototype second-generation coated conductors. We apply our theory using the Kim model, $J_{pK}(B) = J_{pK}(0)/(1 + |B|/B_0)$, as an example. We calculate $J_c(B_a)$ as a function of a perpendicular applied magnetic induction B_a and show how $J_c(B_a)$ is related to $J_{pK}(B)$. We find that $J_c(B_a)$ is very nearly equal to $J_{pK}(B_a)$ when $B_a \geq B_a^*$, where B_a^* is the value of B_a that makes the net flux density zero at the strip's edge. However, $J_c(B_a)$ is suppressed relative to $J_{pK}(B_a)$ at low fields when $B_a < B_a^*$, with the largest suppression occurring when B_a^*/B_0 is of order unity or larger.

PACS numbers: 74.78.-w,74.25.Ha,74.25.Op

I. INTRODUCTION

One of the most important physical properties characterizing a type-II superconductor is its transport critical current I_c. When the current I in a superconducting strip exceeds I_c, a voltage appears along the length; this voltage is due to the motion of vortices or antivortices across the strip. Applying a magnetic induction $\boldsymbol{B}_a$ perpendicular to the current generally decreases I_c, and another important physical property is the strength of the field dependence of $I_c(\boldsymbol{B}_a)$ vs $\boldsymbol{B}_a$. For applications it is of course desirable that this field dependence be as weak as possible, so that I_c remains large in high fields. In low applied fields, the self-field generated by the current through the superconductor also suppresses the critical current. It is the purpose of this paper to present a method by which such self-field effects can be analyzed and calculated.

The geometry of interest here is that of a long type-II superconducting strip of rectangular cross section sketched in Fig. 1. The strip is centered on the z axis and is of width $2a$ along the x direction and thickness $2b$ along the y direction. For simplicity we assume that the thickness is somewhat larger than the London weak-field penetration depth λ, such that (a) the sample dimensions determine the vortex nucleation conditions and (b) we can use macroscopic thermodynamics, which involve the magnetic induction $\boldsymbol{B}$, a local average of the microscopic magnetic induction over a few intervortex spacings, and the corresponding thermodynamic magnetic field $\boldsymbol{H} = \boldsymbol{\nabla}_{\boldsymbol{B}} F(\boldsymbol{B})$, where $F(\boldsymbol{B})$ is the Helmholtz free energy density in the mixed state.[2] When a magnetic induction $\boldsymbol{B}_a$ is applied perpendicular to the z axis, $\boldsymbol{B}$ and $\boldsymbol{H}$ have only x and y components, which depend only on the coordinates x and y. We focus our attention on dimensions of greatest interest to those involved in research and development on second-generation coated conductors [highly oriented YBCO ($YBa_2Cu_3O_{7-\delta}$) films on textured substrates]: YBCO thicknesses in the range 0.2-4 μm and widths in the range 0.1-10 mm, such that $b \ll a$.

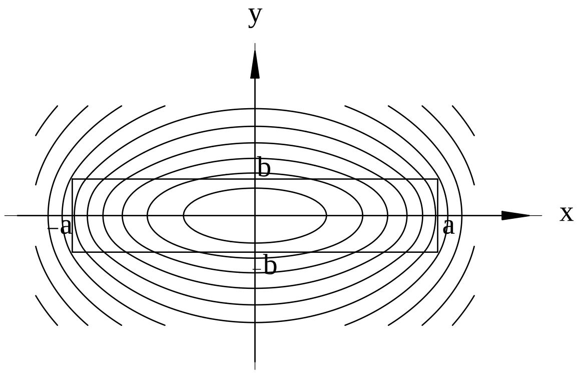

FIG. 1: Superconducting strip of rectangular cross section considered in this paper. Also shown are contours of constant vector potential $\boldsymbol{A}$, which correspond to field lines of $\boldsymbol{B}$, when the strip carries a uniform current density.

Our paper is organized as follows. In Sec. II, we discuss the complications arising when both bulk and edge pinning are present, but we show that bulk pinning dominates over geometrical edge-barrier effects in state-of-the-art YBCO films and prototype second-generation coated conductors. In Sec. III, we discuss the general problem of how to calculate the average critical current density $J_c(\boldsymbol{B}_a)$ in an applied magnetic induction $\boldsymbol{B}_a$ when the local depinning critical current density J_p depends upon the local magnetic induction $\boldsymbol{B}(x,y) = \hat{x}B_x(x,y) + \hat{y}B_y(x,y)$. In Sec. III A, we give some basic equations, and in Sec. III B, we outline, but do not apply, a general method requiring a two-dimensional (2D) grid. In Sec. III C, we develop a general method for calculating $J_c(B_a)$ that uses only a 1D grid but requires the integral of $1/J_p(B_x,B_y)$ with respect to B_x. This method accounts for the spatial variation of $\boldsymbol{B}(x,y)$ and $J_p(\boldsymbol{B})$ over the entire cross section of the film. In Sec. III D, we apply this method for perpendicular applied fields $\boldsymbol{B}_a = \hat{y}B_a$ using the Kim model,[1] $J_{pK}(B) = J_{pK}(0)/(1+|B|/B_0)$, which assumes that J_p depends only upon the magnitude of $\boldsymbol{B}(x,y)$. We calculate $J_c(B_a)$ vs B_a and the field and current distributions across the strip. We briefly summarize our findings in Sec. IV.

II. BULK VS EDGE PINNING

According to critical-state theory in the mixed state of type-II superconductors,[2] at the critical current of a superconducting strip the magnitude of the current density $\boldsymbol{J}(x,y) = J_z(x,y)\hat{z} = \boldsymbol{\nabla}\times\boldsymbol{H}(x,y)$ in a region containing vortices is locally equal to the critical depinning current density $J_p(\boldsymbol{B})$. $J_p(\boldsymbol{B})$ characterizes the bulk pinning force per unit length f_p on a vortex but is defined to have dimensions of current density: $f_p = J_p\phi_0$, where $\phi_0 = h/2e$ is the superconducting flux quantum. On the other hand, the actual current density (averaged over a few intervortex spacings) is $\boldsymbol{j}(x,y) = j_z(x,y)\hat{z} = \boldsymbol{\nabla}\times\boldsymbol{B}(x,y)/\mu_0$, and it is this current density that enters into the Biot-Savart expression from which the self-field contribution to $\boldsymbol{B}$ can be calculated throughout all space.

Depending upon the magnitude of J_p, the magnetic-flux-density and current-density distributions in a superconducting strip can be surprising complicated because of the influence of geometrical edge barriers, Bean-Livingston surface barriers, or surface-barrier effects.[3–20]

For small J_p, the self-field critical current of a superconducting strip is determined entirely by the geometrical edge barrier. For a sample in the Meissner state subjected to an increasing current I in the z direction in the absence of a perpendicular applied field, the current density in the strip averaged over the thickness is[17,21]

$$j_z(x) = \frac{I}{2\pi b\sqrt{a^2-x^2}}, \tag{1}$$

and the y component of the self-field in the plane $y=0$ is[17,21]

$$\begin{aligned} H_y(x,0) &= 0, |x|<a, &(2)\\ &= \frac{xI}{2\pi|x|\sqrt{x^2-a^2}}, |x|>a, &(3)\end{aligned}$$

to good approximation except within about b of the edges at $x=\pm a$. Irreversible vortex penetration occurs and the critical current is reached when $|H_y(\pm a,0)|$ first reaches the barrier-penetration field H_s. In the absence of a Bean-Livingston barrier, $H_s = H_{c1}$, the lower critical field, but in the presence of a Bean-Livingston barrier, H_s may be much larger, even approaching the bulk thermodynamic critical field H_c.[3,22–25] However, the value of H_s and the process by which irreversible penetration first occurs depend sensitively upon the local structure of the edge.[9,11–14,17,18,26–31] The edge-barrier critical current in zero external magnetic field I_{s0} can be estimated by evaluating Eq. (3) at $x\approx a+b/2$, which leads to the result $I_{s0} = 2\pi\sqrt{ab}H_s$ obtained in Ref. 17 for films with rounded edges.[32] Note that when $I = I_{s0}$, the magnitude of the self-field in the middle of the top and bottom surfaces is $|H_x(0,\pm b)| = I_{s0}/2\pi a = \sqrt{b/a}H_s$, which is much smaller than H_s when $b \ll a$, the case of interest here.

When the current I rises slightly above I_{s0}, vortices and antivortices nucleate on opposite sides of the strip and then experience a Lorentz driving force per unit length of magnitude $f_d(x) = j_z(x)\phi_0$, which is sharply peaked at the edges and reaches a minimum at the center of the strip [see Eq. (1)]. Let us consider the case for which the bulk-pinning current density J_p is independent of B (the Bean-London model[33,34]). When J_p is less than $I_{s0}/2\pi ab$, the driving forces exceed the bulk-pinning forces for all x, and the nucleated vortices and antivortices are driven towards each other until they annihilate. We therefore see that the self-field critical current I_c of the strip is governed entirely by the edge barrier, i.e., $I_c = I_{s0}$, independent of the bulk-pinning J_p, when the ratio $p = I_p/I_{s0}$ is less than $2/\pi$, where $I_p = 4abJ_p$ is defined to be the bulk-pinning critical current in the absence of the edge barrier.

For larger values of J_p, i.e., for $p > 2/\pi$, the critical current I_c of the strip (where a voltage first appears along the length) is larger than the current I_{s0} when vortices are first nucleated. As the current I slightly exceeds I_{s0}, the large screening currents near the sample edges drive nucleating vortices and antivortices toward the center of the strip, but they stop where $j_z(x) = J_p$. As shown in Ref. 19, further increases of the current produce metastable magnetic-flux distributions initially characterized by five zones. Near the edges are two vortex-free zones where the local current density $j_z(x) > J_p$. Along the centerline is another vortex-free zone where $j_z(x) < J_p$. On the right side of the central vortex-free zone is a region containing vortices with magnetic flux density $B_y(x) > 0$, in which $j_z(x) = J_p$; and on the left side of the central vortex-free zone is a region containing antivortices with magnetic flux density $B_y(x) < 0$ in which $j_z(x) = J_p$. The critical current I_c is reached when I and $j_z(x)$ are just large enough to drive the vortex-filled and antivortex-filled regions together, shrinking the central vortex-free zone to zero width, such that vortex-antivortex annihilation can occur along the centerline.

In zero applied field when p is just above $2/\pi$, the state of the strip when I is barely above the critical current I_c therefore can be described qualitatively in terms of four zones as follows: Vortices and antivortices nucleate at opposite edges of the strip, where the magnitude of the local magnetic field is equal to H_s. Once nucleated, vortices (antivortices) move rapidly to the left (right) through otherwise vortex-free zones near the strip edges where the supercurrent density $j_z(x)$ exceeds the bulk zero-field depinning critical current density J_p. The vortices (antivortices) then enter a vortex-filled zone on the right (left) side of the centerline, where the magnetic flux density $B_y > 0$ ($B_y < 0$) and the local critical current density $j_z(x)$ is just barely above the depinning critical current density J_p. The critical current I_c is larger than I_{s0} but also larger than I_p because $j_z(x) > J_p$ in the vortex-free zones. Analytic expressions from which I_c can be calculated are given in Refs. 19 and 20 for the case that J_p is independent of B.

For increasing values of J_p or $p = I_p/I_{s0}$, the vortex-free zones at $I = I_c$ become narrower, and they shrink to zero width when the magnitude of the J_p-generated self-field at the sample edges becomes equal to H_s. If J_p is independent of B and $b \ll a$, the self-field at $(x, y) = (\pm a, 0)$ can be shown from Eq. (9) to be

$$H_y(\pm a, 0) = \pm(J_p b/\pi)[\ln(2a/b) + 1] \tag{4}$$

with correction terms inside the brackets of order $(b/a)^2$. The value of J_p that makes $H_y(a, 0) = H_s$ is $J_{ps} = \pi H_s/b[\ln(2a/b) + 1]$, and the corresponding value of p is

$$p_s = \frac{I_{ps}}{I_{s0}} = \frac{2\sqrt{a/b}}{\ln(2a/b) + 1}, \tag{5}$$

where $I_{ps} = 4abJ_{ps}$.

For larger values of the depinning critical current density, $J_p > J_{ps}$ or $p \geq p_s$, the critical current is given by $I_c = I_p$ to excellent approximation because $J_z(x) = J_p$ throughout the entire width of the strip except very near the edges. Any surface-current contribution at the edges arising from a surface-barrier-induced discontinuity in H can be shown to be smaller than I_c by a factor of order b/a.

Such complicated magnetic-field and current-density distributions arising from the geometrical edge barrier are important for strips fabricated of low-pinning superconductors, such as Bi-2212. On the other hand, for state-of-the-art YBCO films and prototype second-generation coated conductors, the depinning critical current density is so high that the parameter p is well above p_s, and the excess current due to the edge barrier is negligible. For example, Rupich et al.[35] recently reported measurements of a self-field critical current of $I_c = 112$ A at 77 K for a coated conductor composite of length 1.25 m and width 1 cm, in which the superconductor was metal-organic-derived YBCO of thickness 0.8 μm coated on a deformation-textured NiW alloy substrate buffered with Y_2O_3/YSZ/CeO_2. We can estimate I_{s0} as follows. The authors of Ref. 36 found from magnetization measurements, using a $1 - (T/T_c)^2$ temperature dependence for $H_c(T)$, $\sqrt{2}H_c(0) = 1.4\times10^4$ Oe, $\kappa = 57$, and $T_c = 93.9$ K for a YBCO single crystal, which yields $H_c = 3.24$ kOe $= 2.6\ \times10^5$ A/m at $T = 77$ K. Taking the nucleation field H_s to be the same as H_{c1} and using the Ginzburg-Landau expression $H_{c1} = (H_c/\kappa\sqrt{2})(\ln\kappa + 0.5)$, we obtain $H_s = H_{c1} = 180$ Oe $= 1.5 \times 10^4$ A/m and $I_{s0} = 4.1$ A. Taking $I_p = I_c = 112$ A, we obtain $p = I_p/I_{s0} = 27$, such that $p \gg p_s$, where $p_s = 3.1$ [Eq. (5)]. This indicates that the vortex-filled region in which the current density is at the depinning critical current density fills practically the entire cross section at the critical current of coated conductors such as that reported in Ref. 35.

III. BULK PINNING

For the remainder of this paper, we limit our attention to materials in which the depinning critical current density is so high that geometrical edge barriers have a negligible effect upon the critical current. We now focus on the questions of how to calculate the the average critical current density $J_c = I_c/4ab$ in an applied magnetic induction $\boldsymbol{B}_a$ and how to determine the magnetic-field and current-density distributions at J_c when the local depinning critical current density J_p has a significant dependence upon the local magnetic induction $\boldsymbol{B}$.

A. Basic equations

Consider a type-II superconducting strip with a geometry as sketched in Fig. 1. If the current density associated with the magnetic induction $\boldsymbol{B} = \boldsymbol{\nabla} \times \boldsymbol{A}$ is $\boldsymbol{j}(x, y) = (1/\mu_0)\boldsymbol{\nabla} \times \boldsymbol{B}(x, y)$, the vector potential $\boldsymbol{A}(x, y) = \hat{z}A_z(x, y)$ generated by $\boldsymbol{j}(x, y)$ can be calculated from

$$A_{zr}(x, y, a, b) = \\ -\frac{\mu_0}{4\pi}\int_{-a}^{a}\int_{-b}^{b} j_z(u, v)\ln[(x-u)^2 + (y-v)^2]dudv, \tag{6}$$

where the subscript r refers to the rectangular cross section. If $\boldsymbol{j} = \hat{z}j_z$ and the sheet current density $K_z = 2bj_z$ are constant over the cross section of the strip, the resulting vector potential and the x and y components of the magnetic induction are

$$A_{zr}(x, y, a, b) = (\mu_0 K_z/2\pi)a_{zr}(x, y, a, b), \tag{7}$$
$$B_{xr}(x, y, a, b) = (\mu_0 K_z/2\pi)b_{xr}(x, y, a, b), \tag{8}$$
$$B_{yr}(x, y, a, b) = (\mu_0 K_z/2\pi)b_{yr}(x, y, a, b), \tag{9}$$

where expressions for the functions a_{zr}, b_{xr}, b_{yr}, and their partial derivatives are given in Appendix A. Shown in Fig. 1 are contours of constant $A_{zr}(x, y)$, which correspond to $\boldsymbol{B}_r$ field lines.

In the limit of vanishing thickness of the strip of width $2a$, simpler results but with singularities at the edges can be obtained by replacing j_z in Eq. (6) by $j_z(x,y) = K_z(x)\delta(y)$, such that the vector potential becomes

$$A_{zs}(x,y,a) = -\frac{\mu_0}{4\pi}\int_{-a}^{a} K_z(u)\ln[(x-u)^2+y^2]du, \quad (10)$$

where the subscript s is a reminder that the results apply to a strip in the limit of zero thickness. If K_z is uniform over the width of the strip, the resulting vector potential and the x and y components of the magnetic induction are

$$A_{zs}(x,y,a) = (\mu_0 K_z/2\pi)a_{zs}(x,y,a), \quad (11)$$

$$B_{xs}(x,y,a) = (\mu_0 K_z/2\pi)b_{xs}(x,y,a), \quad (12)$$

$$B_{ys}(x,y,a) = (\mu_0 K_z/2\pi)b_{ys}(x,y,a), \quad (13)$$

where expressions for the functions a_{zs}, b_{xs}, and b_{ys} are given in Appendix B.

We are interested in calculating the critical current I_c as a function of the applied field when the magnetic induction $\boldsymbol{B}_a$ is applied perpendicular to the z axis. If one equates the current density j_z to the depinning critical current density $J_p(\boldsymbol{B})$ in Eq. (6), which determines the vector potential $\boldsymbol{A}$ describing the self-fields, one must self-consistently determine the spatial variation of the local magnetic induction $\boldsymbol{B} = \boldsymbol{B}_a + \boldsymbol{\nabla}\times\boldsymbol{A}$. In general, $J_p(\boldsymbol{B})$ is not constant over the cross section of the sample, and the critical current density $J_c(\boldsymbol{B}_a) = I_c/4ab$ is therefore not equal to $J_p(\boldsymbol{B}_a)$.

B. General procedure with a 2D grid and $J_p(\boldsymbol{B})$

The following general numerical procedure, which is similar to that used by previous authors[37,38] for the disk geometry, could be used to account for self-field effects when the depinning critical current density $J_p(\boldsymbol{B})$ depends upon both the magnitude and direction of the local magnetic induction $\boldsymbol{B}$. Divide the rectangular cross section into $N = N_xN_y$ current elements of dimensions $\Delta x \times \Delta y$, where $\Delta x = 2a/N_x$ and $\Delta y = 2b/N_y$, centered at the coordinates (x_n, y_n), where $n = 1, 2, ..., N$. If N is large, the bulk-pinning critical current density $J_p(\boldsymbol{B}_n)$ in element n is very nearly constant. The local magnetic induction in element n can be expressed as $\boldsymbol{B}_n = \boldsymbol{B}(x_n, y_n) = \boldsymbol{B}_a + \boldsymbol{B}_{self}(x_n, y_n)$, where $\boldsymbol{B}_{self}(x_n, y_n) = \hat{x}B_{self,x}(x_n, y_n) + \hat{y}B_{self,y}(x_n, y_n)$ can be obtained with the help of Eqs. (8) and (9) by summing the contributions from all current elements:

$$B_{self,x}(x,y) = \sum_{m=1}^{N}\frac{\mu_0 K_m}{2\pi}b_{xr}(x-x_m, y-y_m, \frac{\Delta x}{2}, \frac{\Delta y}{2}), \quad (14)$$

$$B_{self,y}(x,y) = \sum_{m=1}^{N}\frac{\mu_0 K_m}{2\pi}b_{yr}(x-x_m, y-y_m, \frac{\Delta x}{2}, \frac{\Delta y}{2}) \quad (15)$$

with $K_m = J_p(\boldsymbol{B}_m)\Delta y$. This results in $2N$ equations, which for each given bulk-pinning critical current density function $J_p(\boldsymbol{B})$ can be solved by iterative methods to obtain the x and y components of the N vectors $\boldsymbol{B}_n$. The average critical current density can then be calculated as follows:

$$J_c(\boldsymbol{B}_a) = \frac{1}{N}\sum_{n=1}^{N} J_p(\boldsymbol{B}_n). \quad (16)$$

C. General procedure for strips with a 1D grid and $J_p(B_x, B_y)$

Suppose the strip is subjected to a uniform applied magnetic induction $\boldsymbol{B}_a = \hat{x}B_{ax} + \hat{y}B_{ay}$. We consider the case in which the underlying depinning critical current density $J_p(B_x, B_y)$ is a known function of both the x and y components of the local magnetic induction $\boldsymbol{B}$. For example, $J_p(B_x, B_y)$ could be determined experimentally by (a) measuring J_c in applied fields $\boldsymbol{B}_a$ large enough that the effects of the self-field $\boldsymbol{B}_{self}$ are negligible and (b) fitting to a model that allows extrapolation to small B. In calculating the remanent magnetization of disks in self-fields, the authors of Refs. 37 and 38 found for the disk geometry that the magnitude of $\boldsymbol{B}$ changed so significantly over the disk thickness that the depinning critical current density at the top and bottom surfaces was significantly suppressed relative to that midway between the two surfaces. This suppression of the depinning current density near the top and bottom surfaces must also be taken into account to achieve self-consistent solutions accounting for self-field effects upon the average critical current density $J_c(\boldsymbol{B}_a)$ vs $\boldsymbol{B}_a$ of long strips.

There are three properties of thin superconducting strips with $b \ll a$ (see Fig. 1) that enable us to accomplish this using only a 1D grid by applying an idea from Refs. 38 and 39. We simplify the general procedure outlined in Sec. III B by taking $N_y = 1$, such that $N = N_x$, and by considering current elements of dimensions $\Delta x = 2a/N$ and $\Delta y = 2b$, centered at the coordinates $(x_n, 0)$, where $n = 1, 2, ..., N$. For simplicity, we use the approximation that $\boldsymbol{B} \approx \mu_0\boldsymbol{H}$, such that $\boldsymbol{J} \approx \boldsymbol{j} = (1/\mu_0)\boldsymbol{\nabla}\times\boldsymbol{B}$.

The first important property of thin strips we use is that the x and y components of $\boldsymbol{B}_{self}(x,y)$ can be obtained to good accuracy by writing

$$B_{self,x}(x,y) = \sum_{m=1}^{N}\frac{\mu_0 K_m}{2\pi}b_{xr}(x-x_m, y, \frac{\Delta x}{2}, b), \quad (17)$$

$$B_{self,y}(x,y) = \sum_{m=1}^{N}\frac{\mu_0 K_m}{2\pi}b_{yr}(x-x_m, y, \frac{\Delta x}{2}, b), \quad (18)$$

where $K_n = 2b\bar{j}_z(x_n)$ is the average sheet current density in the element at $x = x_n$. The net magnetic induction is $\boldsymbol{B} = \boldsymbol{B}_a + \boldsymbol{B}_{self}$, where

$$B_x(x,y) = B_{ax} + B_{self,x}(x,y), \quad (19)$$

$$B_y(x,y) = B_{ay} + B_{self,y}(x,y). \quad (20)$$

As can be seen from Fig. 1, $B_{self,x}(x,-b) > 0$ and $B_{self,x}(x,b) = -B_{self,x}(x,-b)$.

The second property of thin films we use is that, although the current density $\boldsymbol{j}(x,y) = j_z(x,y)\hat{z}$ is given in general by $j_z = (1/\mu_0)(\partial B_y/\partial x - \partial B_x/\partial y)$, it is a good approximation for most of the strip width to write $j_z = -(1/\mu_0)\partial B_x/\partial y$ when $b \ll a$. The accuracy of this approximation can be estimated for a uniform current density in a strip of rectangular cross section by calculating the ratio $R_J(x,y) = (\partial B_y/\partial x)/(-\partial B_x/\partial y)$ using Eqs. (A6) and (A7). Although $R_J \sim 1$ at the edges of the strip, we find that $R_J(0,0) \approx (2/\pi)(b/a)$ at the center of the strip when $b/a \ll 1$. When $b/a = 0.01$, $R_J(0,0) = 0.0064$ and $R_J(x,0) < 0.1$ for $a - |x| > 3.5b$. When $b/a = 0.001$, $R_J(0,0) = 0.00064$ and $R_J(x,0) < 0.1$ for $a - |x| > 3.5b$.

The third property of thin films we use is that $|\partial B_y/\partial y| \ll |\partial B_x/\partial y|$, such that although $B_x(x,y)$ changes considerably over the film thickness, $B_y(x,y)$ is very nearly a constant, equal to $B_y(x,0)$. The accuracy of this approximation can be estimated for a strip carrying a uniform current density by calculating the ratio $R_B(x) = |[B_y(x,b) - B_y(x,0)]/B_y(x,0)]$ using Eq. (A3). Although $R_B(x)$ is largest near the edges of the strip, $R_B(x) < 0.01$ for $a - |x| > 3.5b$ when $b/a \le 0.01$.

The second property allows us to obtain the average of $j_z(x,y)$ over the sample thickness from $\bar{j}_z(x) = B_{self,x}(x,-b)/\mu_0 b$, and the third property allows us to set $B_y(x,y) = B_y(x,0)$ in the critical state force-balance expression

$$j_z(x,y) = J_p(B_x(x,y), B_y(x,y)), \qquad (21)$$

such that in Eqs. (17) and (18) we may write

$$K_n = 2b\bar{j}_z(x_n) = 2B_{self,x}(x_n,-b)/\mu_0, \qquad (22)$$

where $B_{self,x}(x_n,-b)$ is obtained either numerically or analytically from (see Refs. 38 and 39)

$$\int_{B_{ax}-B_{self,x}(x_n,-b)}^{B_{ax}+B_{self,x}(x_n,-b)} \frac{du}{J_p(u, B_y(x_n,0))} = 2\mu_0 b. \qquad (23)$$

One may now use the above equations to find self-consistent solutions for $\boldsymbol{B}$ and $\boldsymbol{j}$. The $2N$ unknowns, $B_x(x_n,-b)$ and $B_y(x_n,0)$, can be obtained numerically from $2N$ equations obtained from Eqs. (18-20), (22), and (23). Once these solutions have been found, we may calculate the average critical current density from

$$J_c(B_a) = \frac{1}{N}\sum_{n=1}^{N} \bar{j}_z(x_n) = \frac{1}{N\mu_0 b}\sum_{n=1}^{N} B_{self,x}(x_n,-b). \qquad (24)$$

D. Calculations in a perpendicular field with a 1D grid and a Kim-model $J_p(B(x,y))$

We have applied the numerical procedure described in Sec. III C to calculate $J_c(B_a)$ in a perpendicular field $\boldsymbol{B}_a = \hat{y}B_a$ for three ficticious YBCO samples (a, b, and c) with dimensions as in Fig. 1 but with $a = 120$ μm and $b =$ (a) 0.1 μm, (b) 0.5 μm, and (c) 1.5 μm. Suenaga et al.[40] reported that the depinning critical current densities inferred from 77 K magnetization measurements on three YBCO disks with these thicknesses were well fit by the Kim model,[1]

$$J_{pK}(B) = J_{pK}(0)/(1 + |B|/B_0), \qquad (25)$$

except at low fields where self-field effects are responsible for deviations. For $J_p(B_x, B_y)$ in Eq. (23) we therefore took the local depinning critical current density to be $J_p(B_x,B_y) = J_{pK}(B)$, where $B = \sqrt{B_x^2 + B_y^2}$. The parameters were (a) $J_{pK}(0) = 4.32 \times 10^6$ A/cm^2 and B_0 = 17.6 mT, (b) $J_{pK}(0) = 3.22 \times 10^6$ A/cm^2 and B_0 = 18.8 mT, and (c) $J_{pK}(0) = 2.55 \times 10^6$ A/cm^2 and B_0 = 22.6 mT, respectively.[40] With Eq. (25) giving the explicit form for J_p, it was possible to evaluate Eq. (23) analytically with the result

$$\begin{aligned} &2B_0 B_x(x_n,-b) + B_x(x_n,-b)\sqrt{B_x^2(x_n,-b) + B_y^2(x_n,0)} \\ &+ B_y^2(x_n,0)\sinh^{-1}[B_x(x_n,-b)/|B_y(x_n,0)|] \\ &= 2\mu_0 J_{pK}(0) B_0 b. \end{aligned} \qquad (26)$$

Using Mathematica,[41] we solved Eqs. (18-20), (22), and (26) numerically with $N = 101$ to obtain $B_x(x_n,-b)$ and $B_y(x_n,0)$ for samples a, b, and c. This allowed us to calculate $B_x(x,y)$ and $B_y(x,y)$ from Eqs. (17), (18), (22), and

$$B_x(x,y) = B_{self,x}(x,y), \qquad (27)$$

$$B_y(x,y) = B_a + B_{self,y}(x,y). \qquad (28)$$

We also calculated B_a^*, the value of B_a at which $B_y(-a,0) = 0$, for the three samples considered in this paper: $B_a^*/B_0 =$ (a) 0.651, (b) 1.320, and (c) 1.834 or $B_a^* =$ (a) 11.5 mT, (b) 24.8 mT, and (c) 41.4 mT. Shown in Fig. 2 are values of $J_c(B_a)$ vs B_a calculated from Eq. (24). When $B_a \ge B_a^*$, the calculated values of $J_c(B_a)$ agreed with $J_{pK}(B_a)$ within (a) 0.6%, (b) 1.3%, and (c) 2.1% for the three samples, where the values of B_a^* are shown by the solid symbols. Note that the suppression of $J_c(0)$ is greatest for the thickest film. In general, self-field effects become more important as the strip thickness increases.

Shown in Fig. 3 are normalized plots of $B_y(x,0)$ vs x/a for the thickest of the three samples for applied fields $B_a =$ (a) 0, (b) $B_a^*/2$, (c) B_a^*, and (d) $3B_a^*/2$. Note that $B_y = 0$ at the left edge of the sample when $B_a = B_a^*$. Shown in Fig. 4 are corresponding normalized plots of

$$\bar{j}_z(x) = B_x(x,-b)/\mu_0 b \qquad (29)$$

vs x/a. Note that $\bar{j}_z(x)$ is largest at those values of x where $B_y(x,0) = 0$ in Fig. 3. Note also that when $B_a > B_a^*$, $\bar{j}_z$ vs x becomes flatter; this is another indication

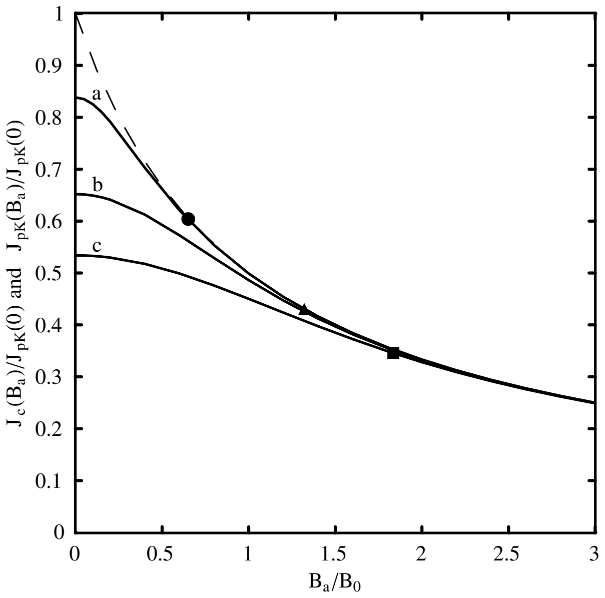

FIG. 2: The normalized average critical current density $J_c(B_a)/J_{pK}(0)$ vs B_a/B_0 calculated from Eq. (24) for the three samples a, b, and c (solid), compared with the Kim model, $J_{pK}(B_a)/J_{pK}(0)$, Eq. (25) (dashed). The values of B_a^*/B_0 for the three samples are identified by the (a) solid circle, (b) solid triangle, and (c) solid square.

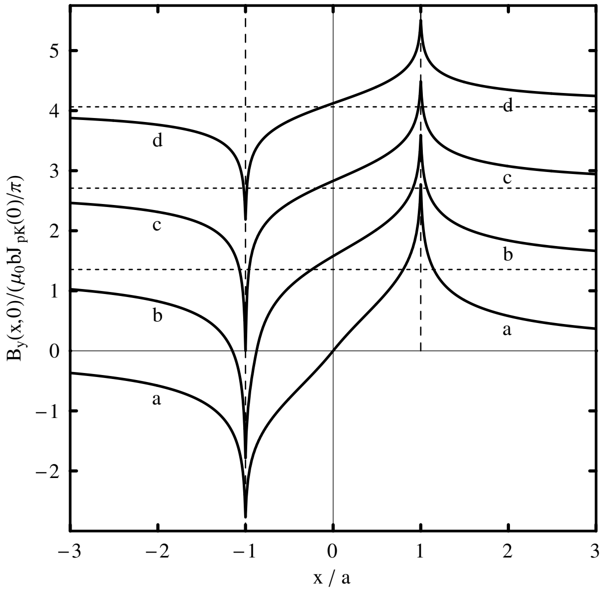

FIG. 3: Normalized magnetic flux density $B_y(x,0)$ vs x/a for the thickest of the three samples, calculated from Eq. (28), for applied fields $B_a =$ (a) 0, (b) $B_a^*/2$, (c) B_a^*, and (d) $3B_a^*/2$ (applied fields shown as horizontal dashed lines), where $B_a^* =$ 41.4 mT and $B_a^*/(\mu_0 bJ_{pK}(0)/\pi) = 2.71$.

that self-field effects have less of an effect upon $J_c(B_a)$ as B_a increases.

A rough (within about a factor of 1.2) estimate of B_a^*, perhaps useful in the analysis of experiments, is $\mu_0 H_y(a,0)$, where J_p in Eq. (4) is replaced by the experimental value of $J_c(0)$. Using the solid curves in Fig. 2 to obtain such an estimate yields (a) 12.7 mT, (b) 30.1 mT, and (c) 49.6 mT for the three samples discussed above, for which $J_c(0)/J_{pK}(0) =$ (a) 0.838, (b) 0.652, and (c) 0.534, or $J_c(0) =$ (a) 3.62 $\times 10^6$ A/cm^2, (b) 2.10 $\times 10^6$ A/cm^2, and (c) 1.36 $\times 10^6$ A/cm^2, respectively.

Several features of the above behavior of J_c vs B_a using the Kim model[1] are close to those found analytically for $J_c(B_a)$ when the applied field is parallel to an infinite slab, as discussed in Appendix C.

IV. SUMMARY

In Sec. II, we briefly reviewed the behavior of the average critical current density $J_c(B_a)$ of superconducting strips when both bulk and edge pinning play a role. The main conclusion of this section is that edge pinning has a negligible effect upon J_c in state-of-the-art YBCO films and prototype second-generation coated conductors.

In Sec. III, we considered the problem of how to account self-consistently for the dependence of the local depinning critical current density upon the local magnetic induction when calculating $J_c(\boldsymbol{B}_a)$. In Sec. III A, we presented some basic equations, and in Sec. III B, we set up, but did not apply, a procedure that, using a 2D grid and starting from an underlying local depinning critical current density $J_p(B_x, B_y)$, would yield the average critical current density $J_c(\boldsymbol{B}_a) = I_c/4ab$ vs an applied magnetic induction $\boldsymbol{B}_a$ for a sample of rectangular cross section of arbitrary width $2a$ and thickness $2b$.

In Sec. III C, we developed a general method that, using a 1D grid and starting from an underlying local depinning critical current density $J_p(B_x, B_y)$, yields the average critical current density $J_c(\boldsymbol{B}_a) = I_c/4ab$ as a function of the magnetic induction $\boldsymbol{B}_a$ applied to a flat sample whose width $2a$ is much larger than its thickness $2b$, a case of considerable interest to those involved in research on prototype second-generation YBCO coated conductors. This method should work well even when J_p is a function of both the magnitude B and the direction $\hat{B}$ of the local magnetic induction $\boldsymbol{B} = B\hat{B}$.

In Sec. III D, we applied the above method to calculate $J_c(B_a)$ in a perpendicular field B_a using the Kim model[1] [Eq. (25)], in which the local depinning critical current density J_p is a function of the magnitude B but not the direction $\hat{B}$ of $\boldsymbol{B} = B\hat{B}$. The functional form of the B dependence of the Kim model's $J_p(B)$ resulted in the particular form of Eq. (26), which we used in determining $B_x(x,-b)$ and $\bar{j}_z(x)$. However, our general method is not limited to the Kim model but could be used with any other realistic model (whether analytic or numerical) for $J_p(B)$. Instead of using Eq. (26), one could use Eq. (23) to obtain a new algorithm connecting $B_x(x_n,-b)$ and $B_y(x_n,0)$ from which $J_c(B_a)$, $B_y(x,0)$, and $\bar{j}_z(x)$ could be determined.

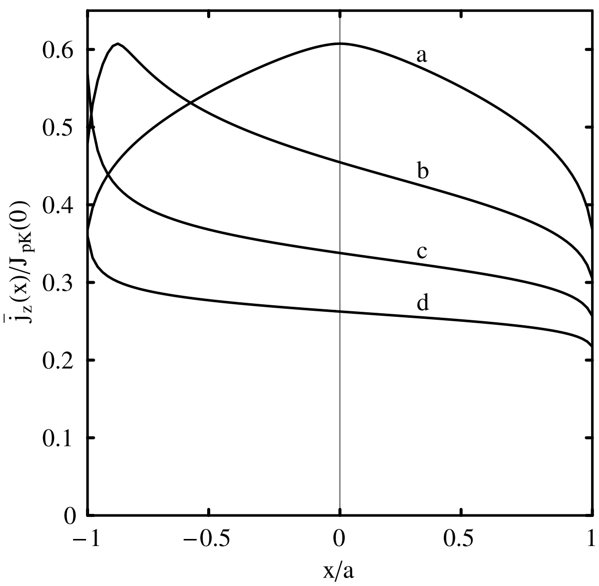

FIG. 4: Local current density averaged over the sample thickness $\bar{j}_z(x)/J_{pK}(0)$ vs x/a for the thickest sample, calculated from Eq. (29) for applied fields $B_a =$ (a) 0, (b) $B_a^*/2$, (c) B_a^*, and (d) $3B_a^*/2$, where $B_a^* = 41.4$ mT.

In this paper we have considered only static current and field distributions at the critical current. For extensive treatments of the dynamics of current and field penetration into strips, see Refs. 39,42–44.

Acknowledgments

We thank E. H. Brandt, S. Foltyn, V. G. Kogan, M. P. Maley, and M. Suenaga for stimulating discussions. This manuscript has been authored in part by Iowa State University of Science and Technology under Contract No. W-7405-ENG-82 with the U.S. Department of Energy.

APPENDIX A: A_z, B_x, AND B_y FOR A STRIP CARRYING UNIFORM SHEET CURRENT DENSITY

When a strip of rectangular cross section (width $2a$ and thickness $2b$) carries a uniform sheet current density $K_z = 2bj_z$ as described in Sec. I, the vector potential derived from Eq. (6) (neglecting an unimportant additive constant) can be expressed as in Eq. (7), where

$$\begin{aligned}
&a_{zr}(x,y,a,b) = \\
&\{(x-a)^2[\arctan(\frac{y+b}{x-a}) - \arctan(\frac{y-b}{x-a})] \\
&+ (x+a)^2[\arctan(\frac{y-b}{x+a}) - \arctan(\frac{y+b}{x+a})] \\
&+ (y-b)^2[\arctan(\frac{x+a}{y-b}) - \arctan(\frac{x-a}{y-b})] \\
&+ (y+b)^2[\arctan(\frac{x-a}{y+b}) - \arctan(\frac{x+a}{y+b})] \\
&+ (x-a)(y+b)\ln[(x-a)^2+(y+b)^2] \\
&- (x-a)(y-b)\ln[(x-a)^2+(y-b)^2] \\
&+ (x+a)(y-b)\ln[(x+a)^2+(y-b)^2] \\
&- (x+a)(y+b)\ln[(x+a)^2+(y+b)^2]\}/4b.
\end{aligned} \tag{A1}$$

The x and y components of the magnetic induction derived from Eq. (7) and $\boldsymbol{B} = \boldsymbol{\nabla} \times \boldsymbol{A}$ are given in Eqs. (8) and (9), where

$$\begin{aligned}
&b_{xr}(x,y,a,b) = \\
&\frac{y-b}{2b}[\arctan(\frac{x+a}{y-b}) - \arctan(\frac{x-a}{y-b})] \\
&+ \frac{y+b}{2b}[\arctan(\frac{x-a}{y+b}) - \arctan(\frac{x+a}{y+b})] \\
&+ \frac{x+a}{4b}\ln[\frac{(x+a)^2+(y-b)^2}{(x+a)^2+(y+b)^2}] \\
&+ \frac{x-a}{4b}\ln[\frac{(x-a)^2+(y+b)^2}{(x-a)^2+(y-b)^2}],
\end{aligned} \tag{A2}$$

$$\begin{aligned}
&b_{yr}(x,y,a,b) = \\
&\frac{x-a}{2b}[\arctan(\frac{y-b}{x-a}) - \arctan(\frac{y+b}{x-a})] \\
&+ \frac{x+a}{2b}[\arctan(\frac{y+b}{x+a}) - \arctan(\frac{y-b}{x+a})] \\
&+ \frac{y-b}{4b}\ln[\frac{(x-a)^2+(y-b)^2}{(x+a)^2+(y-b)^2}] \\
&+ \frac{y+b}{4b}\ln[\frac{(x+a)^2+(y+b)^2}{(x-a)^2+(y+b)^2}].
\end{aligned} \tag{A3}$$

Partial derivatives of the components of $\boldsymbol{B}$, such as $\partial B_{xr}/\partial y = (\mu_0 K_z/2\pi)\partial b_{xr}/\partial y$, are given by the following equations,

$$\partial b_{xr}(x,y,a,b)/\partial x = \ln[\frac{(x+a)^2+(y-b)^2}{(x+a)^2+(y+b)^2}\frac{(x-a)^2+(y+b)^2}{(x-a)^2+(y-b)^2}]/4b, \tag{A4}$$

$$\partial b_{yr}(x,y,a,b)/\partial y = -\partial b_{xr}(x,y,a,b)/\partial x, \tag{A5}$$

$$\begin{aligned}&\partial b_{xr}(x,y,a,b)/\partial y = \\ &[\arctan(\frac{x+a}{y-b}) + \arctan(\frac{x-a}{y+b}) \\ &- \arctan(\frac{x+a}{y+b}) - \arctan(\frac{x-a}{y-b})]/2b,\end{aligned} \tag{A6}$$

$$\begin{aligned}&\partial b_{yr}(x,y,a,b)/\partial x = \\ &[\arctan(\frac{y-b}{x-a}) + \arctan(\frac{y+b}{x+a}) \\ &- \arctan(\frac{y+b}{x-a}) - \arctan(\frac{y-b}{x+a})]/2b.\end{aligned} \tag{A7}$$

APPENDIX B: A_z, B_x, AND B_y FOR A THIN STRIP CARRYING UNIFORM SHEET CURRENT DENSITY

When a thin strip of width $2a$ and negligible thickness carries a uniform sheet current density K_z as described in Sec. I, the vector potential derived from Eq. (10) (neglecting an unimportant additive constant) can be expressed as in Eq. (11), where

$$\begin{aligned}a_{zs}(x,y,a) &= y[\arctan(\frac{x-a}{y}) - \arctan(\frac{x+a}{y})] \\ &+ \frac{x-a}{2}\ln[(x-a)^2+y^2] - \frac{x+a}{2}\ln[(x+a)^2+y^2].\end{aligned} \tag{B1}$$

The x and y components of the magnetic induction derived from Eq. (11) and $\boldsymbol{B} = \boldsymbol{\nabla}\times\boldsymbol{A}$ are given in Eqs. (12) and (13), where

$$b_{xs}(x,y,a) = \arctan(\frac{x-a}{y}) - \arctan(\frac{x+a}{y})], \tag{B2}$$

and

$$b_{ys}(x,y,a) = \frac{1}{2}\ln[\frac{(x+a)^2+y^2}{(x-a)^2+y^2}]. \tag{B3}$$

APPENDIX C: $J_c(B_a)$ FOR B_a PARALLEL TO A SLAB

Although our main interest in this paper is in the average critical current density $J_c(B_a)$ vs B_a when a magnetic field is applied perpendicular to a flat strip, for comparison we present here analytic results for the average critical current density $J_c(B_a)$ in the z direction when a magnetic induction B_a is applied in the y direction parallel to the surface of an infinite slab of thickness $2a$. We consider two models for the depinning critical current density $J_p(B)$ and assume that $B = \mu_0 H$, such that at the critical current we have for each model

$$J_z(x) = J_p(B_y) = \frac{1}{\mu_0}\frac{dB_y(x)}{dx}. \tag{C1}$$

Associated with this current is the self-field B_s, such that $B_y(\pm a) = B_a \pm B_s$. Integrating Eq. (C1) from one side of the slab to the other, we find that the average critical current density is

$$J_c = \frac{B_s}{\mu_0 a}, \tag{C2}$$

where the dependence of B_s upon B_a can be determined by solving Eq. (C1) for $B_y(x)$. For both models of $J_p(B)$, we find that $J_c(B_a)$ has an inflection point at $B_a = B_a^*$ and is equal to $J_p(B_a)$ for $|B_a| \ge B_a^*$.

1. $J_p(B) = \alpha/|B|$

For the model $J_p(B) = \alpha/|B|$, we find that $B_a^* = \sqrt{\mu_0 \alpha a}$ and

$$\frac{J_c(B_a)}{J_c(B_a^*)} = \sqrt{2-(\frac{B_a}{B_a^*})^2}, 0 \le |B_a| \le B_a^*, \tag{C3}$$

$$= \frac{B_a^*}{|B_a|}, |B_a| \ge B_a^*. \tag{C4}$$

2. $J_p(B) = J_{p0}/(1+|B|/B_0)$

For the Kim model[1], $J_p(B) = J_{p0}/(1+|B|/B_0)$, we find that

$$B_a^* = (B_0/2)(\sqrt{1+4\mu_0 J_{p0} a/B_0} - 1) \tag{C5}$$

and

$$\frac{J_c(B_a)}{J_{p0}} = \frac{\sqrt{1+2b^*+2b^{*2}-b^2}-1}{b^*(1+b^*)}, 0 \le b \le b^*, \tag{C6}$$

$$= \frac{1}{1+b}, b \ge b^*, \tag{C7}$$

where $b = |B_a|/B_0$ and $b^* = B_a^*/B_0$.

---

[1] Y. B. Kim, C. F. Hempstead, and A. R. Strnad, Phys. Rev. **129**, 528 (1963).

[2] A. M. Campbell and J. E. Evetts, Adv. Phys. **21**, 199

(1972).

[3] C. P. Bean and J. D. Livingston, Phys. Rev. Lett. **12**, 14 (1973).

[4] J. R. Clem, in *Proceedings of the Conference on Low Temperature Physics* (LT 13), edited by K. D. Timmerhaus, W. J. O'Sullivan, and E. F. Hammel (Plenum, New York, 1974), vol. 3, p. 102.

[5] J. Provost, E. Paumier, and A. Fortini, J. Phys. F **4**, 439 (1974).

[6] A. Fortini and E. Paumier, Phys. Rev. B **14**, 55 (1976).

[7] J. R. Clem, J. Appl. Phys. **50**, 3518 (1979).

[8] A. Buzdin and D. Feinberg, Phys. Lett. A **165**, 281 (1992).

[9] L. Burlachkov, Phys. Rev. B **47**, 8056 (1993).

[10] M. V. Indenbom, H. Kronmüller, T. W. Li, P. H. Kes, and A. A. Menovsky, Physica **222C**, 203 (1994).

[11] Th. Schuster, M. V. Indenbom, H. Kuhn, E. H. Brandt, and M. Konczykowski, Phys. Rev. Lett. **73**, 1424 (1994).

[12] E. Zeldov, A. I. Larkin, V. B. Geshkenbein, M. Konczykowski, D. Majer, B. Khaykovich, V. M. Vinokur, and H. Shtrikman, Phys. Rev. Lett. **73**, 1428 (1994).

[13] M. Benkraouda and J. R. Clem, Phys. Rev. B **53**, 5716 (1996).

[14] T. B. Doyle, R. Labusch, and R. A. Doyle, Physica C **290**, 148 (1997).

[15] D. T. Fuchs at al., Nature **391**, 373 (1998).

[16] D. T. Fuchs at al., Physica C **282**, 2023 (1998).

[17] M. Benkraouda and J. R. Clem, Phys. Rev. B **58**, 15103 (1998).

[18] R. B. Doyle, R. Labusch, and R. A. Doyle, Physica C **332**, 365 (2000).

[19] I. L. Maksimov and A. A. Elistratov, Appl. Phys. Lett. **80**, 2701 (2002).

[20] A. A. Elistratov, D. Yu. Vodolazov, I. L. Maksimov, and J. R. Clem, Phys. Rev. B **66**, 220506(R) (2002); A. A. Elistratov, D. Yu. Vodolazov, I. L. Maksimov, and J. R. Clem, Phys. Rev. B **67**, 099901(E) (2003).

[21] J. R. Clem, R. P. Huebener, and D. E. Gallus, J. Low Temp. Phys. **12**, 449 (1973).

[22] L. Kramer, Z. Phys. **259**, 333 (1973).

[23] H. J. Fink and R. D. Kessinger, Phys. Lett. **25A**, 241 (1967).

[24] P. V. Christiansen and H. Smith, Phys. Rev. **171**, 445 (1968).

[25] H. J. Fink and A. G. Presson, Phys. Rev. **182**, 498 (1969).

[26] J. Z. Sun, W. J. Gallagher, and R. H. Koch, Phys. Rev. B **50**, 13664 (1994).

[27] N. Morozov et al., Physica C **291**, 113 (1997).

[28] R. Labusch and T. B. Doyle, Physica C **290**, 143 (1997).

[29] E. H. Brandt, Phys. Rev. B **59**, 3369 (1999).

[30] E. H. Brandt, Physica B **284-288**,743 (2000).

[31] D. Y. Vodolazov, I. L. Maksimov and E. H. Brandt, Physica C **384** 211 (2003).

[32] Different expressions for I_{s0} were obtained in Refs. 19 and 20, which considered thin films for which $b < \lambda$ and the two-dimensional screening length $\Lambda = \lambda^2/b$ plays an important role.

[33] C. P. Bean, Phys. Rev. Lett. **8**, 250 (1962).

[34] H. London, Phys. Lett. **6**, 162 (1963).

[35] M. W. Rupich, U. Schoop, D. T. Verebelyi, C. Thieme, W. Zhang, X. Li, T. Kodenkandath, N. Nguyen, E. Siegal, D. Buczek, J. Lynch, M. Jowett, E. Thompson, J-S. Wang, J. Scudiere, A. P. Malozemoff, Q. Li, S. Annavarapu, S. Cui, L. Fritzemeier, B. Aldrich, C. Craven, F. Niu, R. Schwall, A. Goyal, and M. Paranthaman, IEEE Trans. Appl. Supercond. **13**, 2458 (2003).

[36] Z. Hao, J. R. Clem, M. W. McElfresh, L. Civale, A. P. Malozemoff, and F. Holtzberg, Phys. Rev. B **43**, 2844 (1991).

[37] M. Däumling and D. C. Larbalestier, Phys. Rev. B **40**, R9350 (1989).

[38] L. W. Conner and A. P. Malozemoff, Phys. Rev. B **43**, 402 (1991).

[39] G. P. Mikitik and E. H. Brandt, Phys. Rev. B **62**, 6800 (2000).

[40] M. Suenaga, Q. Li, Z. Ye, M. Iwakuma, K. Toyota, F. Funaki, S. R. Foltyn, H. Wang, and J. R. Clem, J. Appl. Phys. **95**, 208 (2004) and private communication.

[41] *Mathematica, Version 4.2*, Wolfram Research, Inc., Champaign, IL (2000).

[42] E. H. Brandt, Phys. Rev. B **49**, 9024 (1994).

[43] E. H. Brandt, Phys. Rev. B **54**, 4246 (1996).

[44] E. H. Brandt, Phys. Rev. B **64**, 024505 (2001).